Taylor & Francis
Taylor & Francis Group

Check for updates

Snow Algae Preferentially Grow on Fe-containing Minerals and Contribute to the Formation of Fe Phases

Charity M. Phillips-Lander[a,b]* , Zoe Harrold[a,c]*, Elisabeth M. Hausrath[a] , Antonio Lanzirotti[d], Matthew Newville[d], Christopher T. Adcock[a], James A. Raymond[e], Shichun Huang[a], Oliver Tschauner[a], and Arlaine Sanchez[a]

[a]Department of Geoscience, University of Nevada, Las Vegas, NV, USA; [b]Southwest Research Institute, San Antonio, TX, USA; [c]Desert Research Institute, Reno, NV, USA; [d]Center for Advanced Radiation Sources, University of Chicago, Chicago, IL, USA; [e]School of Life Sciences, University of Nevada, Las Vegas, NV, USA

ABSTRACT

Snow algae growth and mineral dust deposition are both known to strongly decrease snow albedo. Previous work has shown snow algae growth is enhanced in the presence of trace nutrient-containing minerals. Increased dust deposition with acidification due to climate change may therefore additionally enhance snow algae growth. Here we performed batch growth experiments with a snow alga (Chloromonas brevispina) and bacteria co-culture and the minerals andradite ($Ca_{3.0}(Fe_{0.6},Al_{0.43})_2(SiO_4)_3$), olivine ($Mg_{1.8}Fe_{0.2}SiO_4$), and quartz ($SiO_2$), to observe differences in snow algae attachment to mineral surfaces with differing iron (Fe) contents. In the presence of olivine, which has a low Fe content ($\sim$9%), the number of snow algae on the surface of the olivine decreased with decreasing concentrations of snow algae in the medium. In contrast, in the presence of andradite, which has a higher Fe content ($\sim$16%), the number of snow algae on the surface of andradite remained high even when concentrations of snow algae in the medium were greatly decreased. Additionally, μX-ray Fluorescence (μXRF) measurements indicate greater formation of Fe-containing precipitates on the mineral surfaces in the presence of the snow algae cells than in abiotic controls. These results show that the snow alga both preferentially grows on Fe-rich surfaces and forms Fe-containing precipitates, indicating the presence of a potential positive feedback system that could amplify the effect of dust deposition on snow albedo and therefore climate change.

Introduction

Snow and ice cover up to 33% of the Earth on a seasonal basis and thus their albedos can significantly affect climate. Snow albedo is significantly decreased by the deposition of dust (Warren 1984) as well as the growth of snow algae (Benning et al. 2014; Kohshima et al. 1993; Lutz et al. 2014; Thomas and Duval 1995). For example, dense snow algae blooms were shown to decrease the albedo of regions of the Greenland Ice Sheet by one third to one half compared to clean snow (Yallop et al. 2012). Similarly, Stibal et al. (2017) showed that a doubling of snow algae population resulted in an albedo decrease of $3.8 \pm 0.35\%$. Lutz et al. (2016) estimated that the overall decrease in snow albedo by snow algal blooms over one melt season is 13%, and in a region of the Russian Arctic, red snow algae was found to cover 80% of the areas examined (Hisakawa et al. 2015). There is therefore a need to include the effect of snow algae in numerical albedo models (Benning et al. 2014). In order to understand the impact of snow algae on albedo, we must

first understand the factors that control snow algae growth, and how they may change as the planet warms.

Numerous environmental factors impact the extent of snow algae growth. Snow algae blooms are more common in snow containing high amounts of dust, which is thought to provide nutrients to the snow algae populations (Lutz et al. 2015a). The dominant snow algae species in an environment also depends on the amount of liquid water and nutrients available. Chloromonas species, for example, tend to dominate in nutrient-limited environments (Lutz et al. 2015b). Snow algae growth is enhanced by increased carbon dioxide concentrations (Hamilton and Havig 2018). In field manipulations, Ganey et al. (2017) found that adding an aqueous fertilizer containing nitrogen, phosphorus, and potassium increased snow algae counts by a factor of four, and adding liquid water without fertilizer increased snow algae counts by a factor of two. Hodson et al. (2017) also found greater populations of snow algae in coastal Antarctic regions impacted by nutrient input from minerals and marine fauna compared to regions farther inland that lack such

nutrient inputs. Global warming is predicted to increase the amount of mineral dust in the atmosphere due to increasing aridification (Achakulwisut et al. 2018). Increased snow-water and nutrient content from an increased occurrence of dust on snow may facilitate snow algae growth, further affecting snow albedo and snow melt.

Field assessment indicates that the snow associated with snow algae blooms is enriched in nutrients relative to clean snow, which suggests snow algae communities may actively extract and cycle limiting nutrients to support their growth (Hamilton and Havig 2017). Nutrient cycling, particularly organic carbon cycling, by snow algae may also drive subglacial weathering (Havig and Hamilton 2019). Laboratory experiments demonstrated that snow alga growth was enhanced in the presence of olivine ($Mg_{1.8}Fe_{0.2}SiO_4$), and that the dissolution of olivine was also enhanced in the presence of the alga and its associated bacteria (Harrold et al. 2018). Nitrogen-limitation has also been shown to affect the behavior of snow alga (Leya et al. 2009) and their production of metabolites (Lutz et al. 2017). Microorganisms routinely utilize and preferentially colonize minerals to meet their nutrient requirements (Hausrath et al. 2007; Hutchens 2009; Hutchens et al. 2006; Liermann et al. 2007; Roberts 2004; Rogers and Bennett 2004; Song et al. 2007; Suzuki 2001). For example, Fe-reducers were found to preferentially colonize Fe-minerals and Fe-coated glass (Roberts 2004). However, little is known about the direct interactions of snow algae cells with mineral surfaces.

Iron is required for chlorophyll production and electron transport during photosynthesis, making it critically important to photosynthetic organisms (Geider and La Roche 1994; Schoffman et al. 2016). Fe-limitation can negatively impact algal growth by diminishing chlorophyll production (chlorosis), which can reduce energy production efficiency and decrease cell multiplication (Geider and La Roche 1994). Moreover, Fe-limitation also influences microbial community structures, including the algae:prokaryote ratios in marine communities (Geider and La Roche 1994) and snow algae communities (Harrold et al. 2018).

Here, we examined the growth of xenic *Chloromonas brevispina* cultures and the formation of secondary precipitates on polished thin and thick sections of silicate minerals with different iron contents (olivine ($Mg_{1.8}Fe_{0.2}SiO_4$), andradite ($Ca_{3.0}(Fe_{0.6}Al_{0.43})_2(SiO_4)_3$), and quartz ($SiO_2$)). Our observations reveal preferential growth of snow algae on andradite, which has a high iron content ($\sim16\%$), and enhanced formation of Fe precipitates in the presence of snow algae relative to abiotic controls.

Methods

Mineral substrate preparation

San Carlos olivine ($Mg_{1.8}Fe_{0.2}SiO_4$) was obtained from Alfa Aesar, research grade quartz (SiO_2) from Wards Minerals (#495886), and andradite-grossular garnet [$Ca_{3.0}(Fe_{0.6}Al_{0.43})_2(SiO_4)_3$] (Supplemental Table S1, Figure S1) from Garnet Hill, CA from Minerals Unlimited. The Mg-rich San Carlos olivine ($Mg_{1.8}Fe_{0.2}SiO_4$) is referred to

herein as forsterite, and, although it is not the Fe-free Mg-rich end member (containing $\sim 9\%$Fe; Wogelius and Walter 1992), it is of high purity and commonly used in weathering experiments (e.g., Hausrath et al. 2008; Hausrath and Tschauner 2013; Pokrovsky and Schott 2000). Since high purity fayalite is difficult to obtain (Hausrath and Brantley 2010), we used the andradite-grossular garnet ($\sim16\%$ Fe) for a silicate mineral with high-Fe content (McAloon and Hofmeister 1995). Mineral chips were visually picked under a light microscope to ensure few inclusions were present. Some inclusions were, however, detected within the andradite during scanning electron microscopy analysis of andradite surfaces (Supplemental Figure S1). Electron microprobe analysis, using a JEOL JXA-8900 in the Electron Microanalysis Imaging Laboratory (EMiL) at the University of Nevada, Las Vegas (UNLV), indicated that these inclusions are wollastonite with diopside rims (Supplemental Table S1, Figure S1). Both thin and thick sections of each mineral were prepared for incubation and analysis. Duplicate sets of thin sections were mounted and prepared for each mineral: forsterite (F), quartz (Q), andradite (A), and a multimineral mount including all three minerals (FAQ) on 50×25 mm Chemglass quartz glass slides (VWR #80063-856) by National Petrographic Services. An additional set of thin sections was also prepared from epoxy mounts as a mineral-free control. Because thin sections were only polished to 6 μm grit, and were unable to be polished further due to plucking, a set of thick sections was generated from the same billets as the thin sections, but polished to 0.25 μm grit for Scanning Electron Microscopy (SEM) and microprobe analysis.

Each thin and thick section was sterilized in 100% ethanol by sonicating three times, for 1 minute, 30 seconds, and 30 seconds, respectively. The sections were then left submerged in a beaker of 100% ethanol in a laminar flow hood until they were placed in a sterile petri dish with sterilized forceps. Sections were allowed to dry in the covered petri dishes and subsequently submerged with sterile growth medium.

Incubation experiments

Chloromonas brevispina–bacterial co-cultures, hereafter referred to as xenic cultures, were provided by James Raymond, purchased from the Culture Collection of Algae, University of Texas, Austin (UTEX B SNO96 culture). The xenic *C. brevispina* culture was originally collected and isolated by Ronald Hoham from Lac Laflamme, Quebec, Canada (Hoham et al. 1979). Xenic cultures were maintained on M1 growth medium described by Hoham et al. (1979). The M1 growth medium with the 1% v/v trace metal solution was autoclave-sterilized prior to the addition of the vitamin solution (0.1% v/v). The vitamin solution (5 mg mL^{-1} biotin, and 1 mg mL^{-1} vitamin B$_{12}$, and thiamine-HCl) was filter-sterilized (0.2 μm filter) before addition to the autoclave-sterilized M1 medium. Fe-limited M1 medium was prepared without the addition of Fe-EDTA and with a trace metal solution without Fe. Both the full nutrient M1
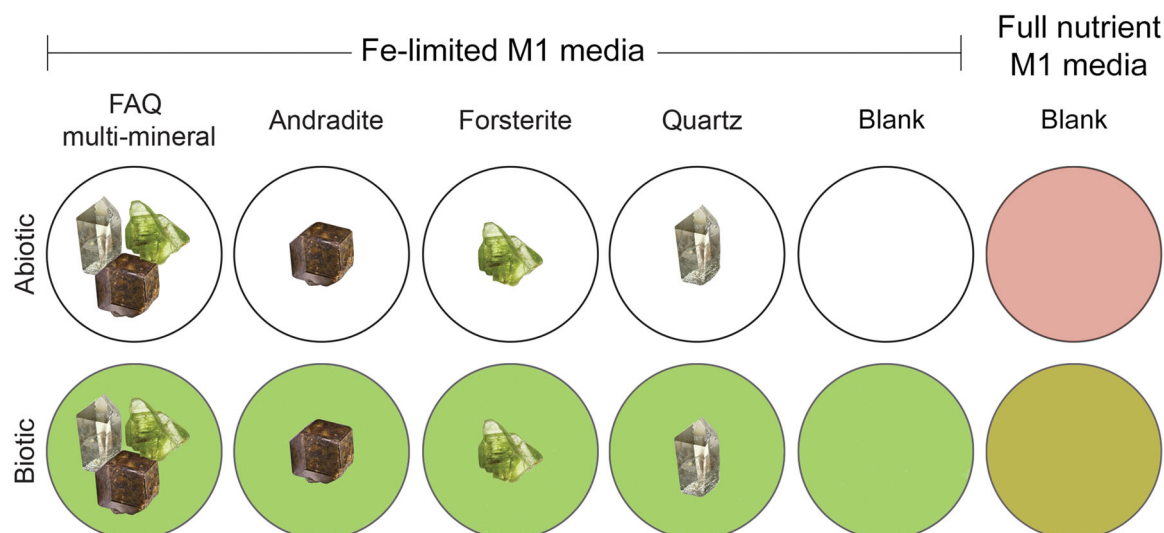
Figure 1. Schematic of the experimental setup of the thin and thick sections, showing the individual (Andradite (A), Forsterite (F), and Quartz (Q) and multi-mineral (Forsterite, Andradite, and Quartz (FAQ)) mineral sections in the presence of the xenic snow algae culture (biotic) and sterile medium (abiotic), as well as the Fe-limiting and full nutrient mineral-free blanks, with and without snow algae. Quartz and olivine images, Rob Lavinsky, iRocks.com, CC-BY-SA-3.0. Andradite image, Didier Descouens, CC-BY SA-4.0.

media and the Fe-limited M1 media had initial pH values of approximately 5.3.

Twenty-four 125 mL flasks of Fe-limited M1 medium and 4 flasks of full nutrient M1 medium were autoclave-sterilized before chilling to 4 °C. One half of the flasks for each medium type were inoculated with 1.25 mL of xenic *C. brevispina* culture in a laminar flow hood and mixed. Sixty mL of the medium, either inoculated or sterile, was then poured over the thin sections in the petri dishes in the laminar flow hood (Figure 1). Each petri dish held 1 thin section. The covered petri dishes were incubated at 4 °C for 30 days, which is the typical time required for the xenic *C. brevispina* culture to reach stationary phase growth (Harrold et al. 2018). When the thin sections were removed they were all still completely submerged in the medium.

To ensure comparable experimental conditions, polished thick sections were submerged with the first of each set of thin sections 8 days after the thin sections were submerged, and removed 9 days after the thin sections were removed. Upon thick section removal, small portions of the quartz and multi-mineral (FAQ) sections reacted under abiotic conditions were exposed to the air. Although the timing is slightly offset between the thin and thick sections, the total duration and incubation conditions are nearly identical, and we make the assumption that the analyses performed only on the polished thick sections (Scanning electron microscopy) or only on the thin sections (surface area determinations and synchrotron analyses) reflect the incubation conditions common to both the thin and thick sections as measured by the ICP-MS solution compositions and solution cell counts of both snow algae and bacteria. Sterile, culture-free experiments were run in parallel to all xenic *C. brevispina* cultures as abiotic controls, epoxy-only mineral-free incubations were run as mineral-free controls, and Fe-bearing cultures were also grown in parallel as full-nutrient controls (Figure 1).

Solution chemistry

Samples of medium (10 mL each) were collected at the beginning and end (30 day) of the thin-section experiments, filtered through a 0.2 μm filter, preserved with 1% high purity HNO_3, and stored at 4 °C for geochemical analysis. Aqueous Ca, Mg, Fe, and Si were measured using a Thermo Fisher iCAPQ ICP-MS equipped with Qtegra software and an automated sampler at UNLV using matrix-matched standards (Table S2 Supplemental Online Material (SOM)). Solution pH was measured at the beginning of the thin section experiments, and at the end of the thin or thick section experiments, dependent upon replicates (Table 1).

Cell concentrations in medium

Samples of medium for cell counts were collected at the beginning and end of the experiments. Algal cell counting was completed according to Harrold et al. (2018). Briefly, cell count samples were fixed with 1.9% filter-sterilized formaldehyde directly after sample collection and stored at 4 °C before analysis. Fixed samples were resuspended by vortexing, and 10 μL of sample placed in disposable Incyto C-chip hemocytometer chambers (Model #DHC-N01). Algae cells were counted at 400× magnification on an Olympus BH microscope, for low to moderate cell concentrations within each of five large grid zones ($V_{grid,L} = 1 \times 10^{-4}$ mL), and for high cell concentrations in nine to thirteen small central grid zones ($V_{grid,sm} = 4 \times 10^{-6}$ mL). Small or malformed cells were counted separately (SOM Table S3) and are not included in cell concentration data. Concentrations of algal cells were determined according to the following equation:

$$C_{algae} = \frac{N \times D}{n \times V_{grid}}$$

Table 1. pH data.

	pH Initial[a]	Final[a]
Fe-limited; No mineral Supplement		
Abiotic-1	5.33	5.44
Abiotic-2	5.36	5.43
Biotic-1	5.34	5.56
Biotic-2	5.35	5.50
Fe-limited; Forsterite Supplement		
Abiotic-1	5.34	5.40
Abiotic-2	5.35	5.30
Biotic-1	5.85	5.63
Biotic-2	5.36	5.47
Fe-limited; Andradite Supplement		
Abiotic-1	5.34	5.36
Abiotic-2	5.35	5.31
Biotic-1	5.36	5.63
Biotic-2	5.35	5.43
Fe-limited; Quartz Supplement		
Abiotic-1	5.33	5.39
Abiotic-2	5.35	5.28
Biotic-1	5.33	5.57
Biotic-2	5.31	5.42
Fe-limited; Multimineral Supplement		
Abiotic-1	5.37	5.58
Abiotic-2	5.36	5.33
Biotic-1	5.32	5.74
Biotic-2	5.37	5.47
Full Nutrient Media		
Abiotic-1	5.02	5.20
Abiotic-2	5.03	5.20
Biotic-1	5.04	4.55
Biotic-2	5.00	4.49

[a]Initial pH measurements were made at the start of the thin section experiments. Final pH measurements for thin section experiments were taken at 30 days from the start of the thin section experiments for the second set of thin sections indicated with a -2. At the end of the thick section experiments (9 days later), pH was measured from remaining experimental solutions (which had previous contained the first set of thin sections) indicated with a -1

where algae concentration (C_{algae}) is reported in cell mL^{-1}, n is the number of grid blocks counted, N is the total cell count in n blocks, D is the dilution factor due to formaldehyde fixation, and V_{grid} is the grid volume used for enumeration.

Bacteria concentrations were determined by flow cytometry using the BD FACSCalibur Flow Cytometer in the UNLV Genomics Core Facility. Briefly, formaldehyde-preserved samples prepared as described above were filtered through 3 μm polycarbonate filters (Nucleopore part #110612) to remove the snow algae cells. Examination of the filtered solutions via microscopy confirmed that the snow algae were removed. Filtered solutions were diluted either 1:10 or 1:100 for all experiments depending on bacteria concentrations, and 1:1000 for the initial inoculum (see SOM Table 5). The filtered, diluted samples were then stained using the Cell Viability Kit with BD Liquid Counting Beads (BD catalog # 34980), and analyzed with the counting beads to obtain quantitative cell counts. Following the manufacturer's instructions, approximately 1000 bead events were collected for each sample, and cell concentration was then calculated (see SOM).

Examination of mineral surfaces

At the end of the incubation experiments described above, the mineral thin and thick-sections were submerged three times in sterile 18 MΩ cm^{-1} water for 1 minute, 1 minute, and 5 minutes, respectively, to reduce salt precipitation before flash-freezing ($-80\,°C$) for 3 hours. Once frozen, thin and thick sections were freeze dried for 2 hours.

Thick sections were then gold-coated for SEM analysis. Unreacted, abiotically reacted, and biotically reacted forsterite, andradite, and quartz were analyzed at the UNLV EMiL facility using a JEOL field-emission JSM-6700F scanning electron microscope equipped with secondary and backscattered electron (BSE) detectors and an Oxford ISIS EDS system. At least 10 BSE fields-of-view were examined for each thick section to document attachment and colonization of snow algae. Cell densities (cells μm^{-2}) were estimated by counting the total number of algal cells present in 10 fields of view and dividing this value by the total area of all counted fields of view. Secondary precipitates were also observed on mineral surfaces of the polished thick sections. The precipitates were analyzed at the Advanced Photon Source (APS) 13-IDE beamline at Argonne National Laboratory, Chicago, IL to examine the association of snow algae and secondary precipitates in thin section experiments using μX-ray fluorescence (μXRF). μXRF maps were acquired at 18 keV with 2 μm step size and 2 μm spot size using a four-element vortex silicon drift detector. Large maps (300 μm × 300 μm) used a dwell time of 300 ms. Smaller maps (100 μm × 100 μm) were acquired with 500 ms dwell times. Synchrotron transmission μXRD was acquired simultaneously with the μXRF mapping using a Perkin Elmer 1621 amorphous silicon Area Detector.

Results

We conducted biotic and abiotic incubation experiments in duplicate to examine snow algae co-culture growth on Fe-bearing silicate mineral substrates in full-nutrient and Fe-limited media (Figure 1). We compared snow algae growth on individual silicate minerals including quartz (Fe ∼ 0 wt.%), forsterite (Fe ∼ 9 wt. %), and andradite (Fe ∼ 16 wt.%), and in systems containing all three silicate minerals (FAQ) (Figure 1).

Solution chemistry

At the conclusion of the thin section experiments, pH measurements were acquired from solutions that had not contacted thick sections (the second set of thin section experiments). Final pH measurements of solutions for experiments that did contain thick sections (and previously, the first set of thin sections) were measured 9 days later–when those experiments were concluded. In general, pH values increased more in experiments containing biota relative to the abiotic controls (Table 1), with the exception being the full nutrient medium, which had lower pH values than any other condition. Experiments that had contained thick sections showed higher final pH values than those that had not.

Calcium concentrations generally increased over the course of the experiments (SOM Table S2); in contrast Mg

Table 2. C. brevispina algal, and bacterial cell concentrations in medium at end of experiments.

Medium	Minerals present	[algae] (10^5 cell mL^{-1})	[bacteria] (10^7 cell mL^{-1})	algae: bacteria ratio $\times 10^{-2}$
Fe-limited	Andradite-1	8.11	6.91	1.17
Fe-limited	Andradite-2	5.05	4.96	1.02
Fe-limited	Forsterite-1	5.47	1.65	3.32
Fe-limited	Forsterite-2	3.73	4.20	0.89
Fe-limited	Quartz-1	2.29	5.99	0.38
Fe-limited	Quartz-2	4.72	2.68	1.76
Fe-limited	FAQ-1	2.46	4.55	0.54
Fe-limited	FAQ-2	5.89	4.44	1.33
Fe-limited	Epoxy-1	1.55	7.41	0.21
Fe-limited	Epoxy-2	1.26	4.74	0.27
M1	none	5.28	6.96	0.76
M1	none	2.84	5.49	0.52
M1	Innoculum	4.21	7.62	0.55

FAQ: Forsterite, Andradite, and Quartz multi-mineral section, 1 and 2 indicate replicates

and Fe concentrations typically increased in the abiotic mineral-containing solutions and decreased in the biotic mineral-containing solutions. Changes in silica concentrations were variable throughout the experiment. The increase in Ca, Mg, and Fe concentrations in the abiotic Fe-limited solutions that contained epoxy-only mineral-free thin sections suggest that leaching occurred from the epoxy and glass slides as well as the minerals. Decreases observed in the full nutrient medium under abiotic conditions suggest that abiotic precipitation may also occur.

Cell concentrations in medium

C. brevispina cell counts (Table 2) were highest in the presence of the andradite, and lowest in the presence of the epoxy-only supplement. After 30 days incubation, algal cell concentrations in all conditions except the epoxy-only supplement were generally comparable to those in the initial inoculum. In contrast, bacteria concentrations in all conditions were lower than those in the initial inoculum (Table 2). Algae: bacteria ratios were lowest in the epoxy-only slides, indicating the importance of Fe for algal growth.

Attachment to and colonization of mineral surfaces

Snow algae cell concentrations on the mineral surfaces in the multi-mineral (FAQ) condition followed the order andradite > quartz ~ forsterite, indicating that, under identical conditions, algae attachment was highest on the mineral with the highest Fe mineral content (Figure 2). Algal cell concentrations in the medium were approximately twice as large in the forsterite-only experiment relative to the multi-mineral (FAQ) experiment (Table 2). This result was consistent with a similar (~2x) increase of snow algae on the forsterite surface in forsterite-only experiments relative to forsterite surfaces in the FAQ experiment (Figure 3 and Table 3). In contrast, the concentration of snow algae on the andradite surface remained high even when the number of snow algae in the medium decreased by a factor of 3 from the andradite only experiments to the multi-mineral (FAQ) experiments (Figure 3 and Tables 2 and 3).

Algal colonization patterns also differed between andradite, forsterite, and quartz. Algae attached and grew in large masses on andradite, in both multi-mineral and individual mineral experiments. In contrast, algal cells formed smaller clusters in experiments containing only forsterite. Dispersed and isolated cell attachment occurred on quartz surfaces, both in individual mineral and multi-mineral (FAQ) experiments, and on forsterite-surfaces in the multi-mineral (FAQ) experiment. Such differences in growth patterns have been previously termed biovermiculation. Bacterial biovermiculation patterns have been identified at macroscopic scales in cave environments (Jones et al. 2008). Snow algae cells also preferentially adhered to pits in the mineral surfaces (Figure 2), and formed biofilms (Figure 4).

Secondary Fe-Precipitates

Secondary Fe-precipitates were observed on mineral surfaces by SEM in both the presence and absence of snow algae cultures (Figure 4). In multi-mineral (FAQ) thin-section experiments, secondary Fe-precipitates were measured in both abiotic and biotic samples on quartz surfaces by µXRF. However, significantly more Fe-containing precipitates were observed in the biotic experiments (Figure 5). These Fe-containing precipitates were observed in association with the snow algae consortia (Figure 5), which were distinguished by high potassium (K) concentrations in the µXRF data. Synchrotron µXRD measurements of these precipitates indicate that they are poorly crystalline, but consistent with the diffraction pattern of fougerite (SOM Figures S2 and S3). Secondary precipitates were only discernable on quartz due to the absence of Fe in quartz, and could not be measured on the andradite and forsterite samples that contain Fe.

Discussion

Snow algae, which decrease the albedo of snow (Benning et al. 2014; Kohshima et al. 1993; Lutz et al. 2014; Thomas and Duval 1995), have previously been shown to utilize Fe from Fe-bearing minerals to increase and sustain cell growth under otherwise Fe-limiting conditions (Harrold et al. 2018). Increasing aridification due to climate change is expected to increase atmospheric dust (Achakulwisut et al. 2018), which when deposited on snow could provide additional trace nutrients to snow algae.

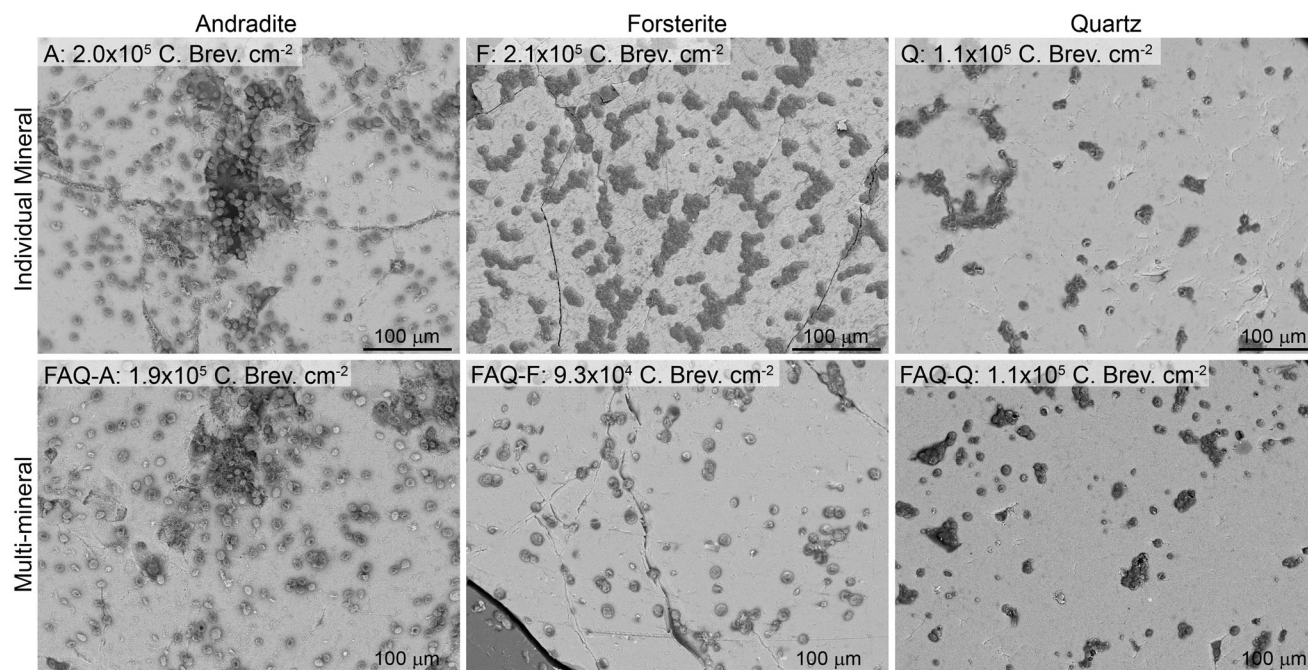In this study, we explored interactions between snow algae and mineral surfaces by incubating C. brevispina and

Figure 2. Scanning electron microscopy image of snow algae cells on mineral surfaces for each mineral in the multi-mineral and individual mineral sections. Algal cell concentrations per surface area are reported on each image. Snow algae cell concentrations on the mineral surfaces in the multi-mineral (FAQ) thick section follow the order andradite > quartz ~ forsterite. This observation indicates that under identical, Fe-limiting conditions, the snow algae preferentially attach to the mineral with the highest Fe content (andradite). In addition, the number of snow algae cells on the forsterite surfaces is greater in the forsterite only condition than in the presence of the other minerals, likely due to the higher concentrations of snow algae cells in the medium (See Figure 3).
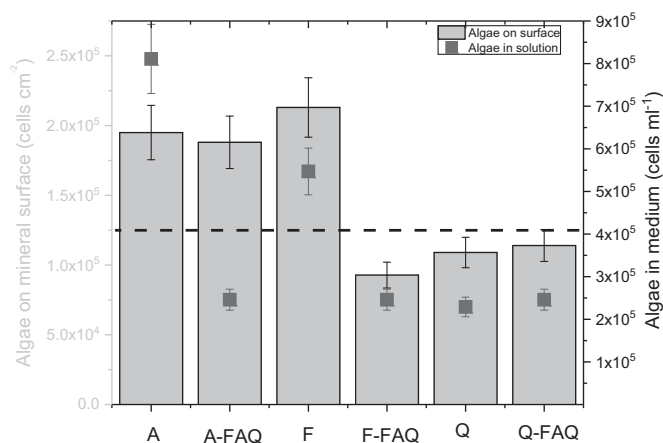

Figure 3. Snow algae concentrations in the medium and on mineral surfaces. Algal attachment to forsterite, a relatively low-Fe mineral, appears linked to the concentration of cells in solution and may be a result of electrostatic interactions. In contrast, attachment to andradite, which contains more Fe per unit cell, remains high even when concentrations of snow algae in the medium are relatively low in the FAQ experiments, suggesting that cells are actively colonizing the mineral surface. These results clearly demonstrate that more snow algae will attach to the high Fe andradite than olivine or quartz when in the presence of medium containing the same algae cell concentration (e.g., the FAQ solutions). The dotted horizontal line indicates the average snow algae cell concentration grown under full nutrient conditions. Uncertainty is estimated as 10% based on Harrold et al. (2018).

Table 3. Algal colonization of mineral surfaces.

Sample	Algae 10^5 cell cm^{-2}
Forsterite	
Multi-mineral	0.928
Single mineral	2.13
Andradite	
Multi-mineral	1.88
Single mineral	1.95
Quartz	
Multi-mineral	1.14
Single mineral	1.09

solution ($\sim 10^5$ cells/ml) is much higher than the number of algal cells on the mineral surfaces, we might expect bulk algae concentration in the medium to control the number of algal cells on the mineral surface. This appears to be the case for the low-Fe mineral forsterite, where concentrations of snow algae on the forsterite surfaces approximately doubled when the concentrations of snow algae in the medium approximately doubled (Figure 3).

This effect may be partly due to electrostatic effects. The point of zero charge (PZC) is approximately pH 10.5 for olivine (forsterite) (Wogelius and Walther 1991), 4.6 for andradite (Khalek and Parekh 2013), and 2.0 for quartz (Stumm and Morgan 1981). At the average final experimental pH of the Fe-limited experiments of approximately 5.5, both andradite and quartz are net negatively charged, forsterite has a net positive charge, and cell surfaces are predicted to have a net negative charge (Jucker et al. 1996). The relatively evenly dispersed nature of snow algae cells on the forsterite surface also supports the potential importance of electrostatic attraction of the snow algae cells to the forsterite surface. Based on electrostatic effects alone, at
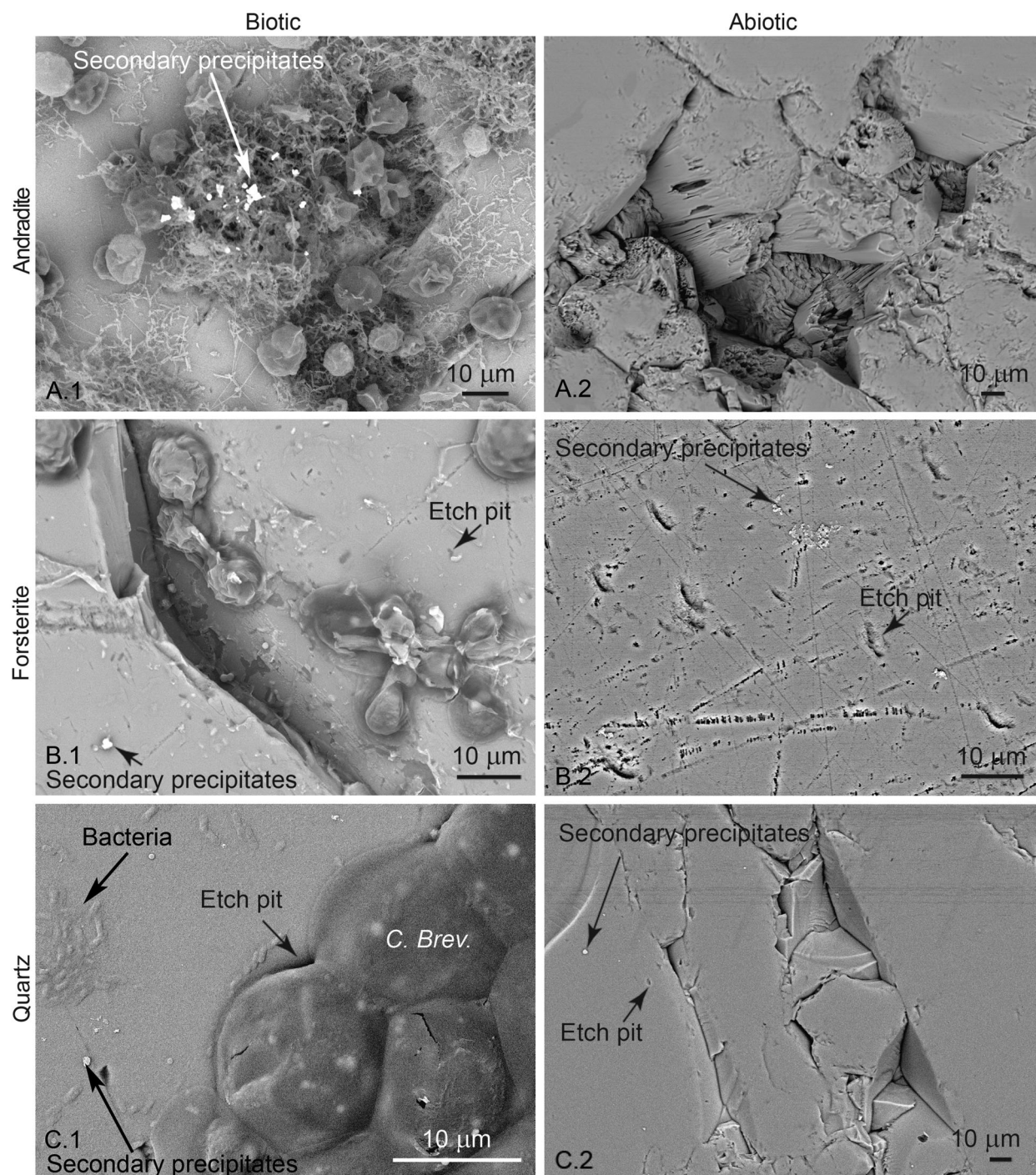
its associated bacteria in the presence of three minerals (forsterite, andradite, and quartz) with different Fe contents, as individual minerals and multimineral thin- and thick-sections. To interpret these interactions, we compared algae concentrations in solution and on the mineral surfaces across mineral incubations and with nutrient-containing and abiotic controls. Since the total number of algal cells in the

Figure 4. Scanning electron microscopy images of the polished thick sections reacted with and without the snow algae cultures. Snow algae and bacteria are attached to the mineral surfaces. Mineral surfaces show effects of polishing and plucking, which is similarly observed with the unreacted phases (Supplemental online material figure 1).

the pH of our experiments we would therefore expect the cell-mineral attachment to occur in the order forsterite > andradite > quartz.

In the multi-mineral (FAQ) condition where each mineral is exposed to the same snow algae concentration in the medium, however, the concentration of snow algae on andradite surfaces was approximately double compared to the concentrations on the quartz and forsterite surfaces. This suggests that snow algae preferentially colonize the andradite because it has the highest concentration of iron,

and that under low Fe growth conditions, snow algae will preferentially attach to minerals with greater Fe content. Snow algae cells also preferentially adhered to mineral pits on the andradite. One possibility is that the pits are rough inside, facilitating adhesion. Another possibility is that the pits have a higher local surface area, and therefore present more Fe at the surface. SEM analyses also show biofilm formation on mineral surfaces (Figure 4), and previous work has shown that nutrient availability can impact the extent of microbial biofilm formation (Dewanti and Wong 1995).
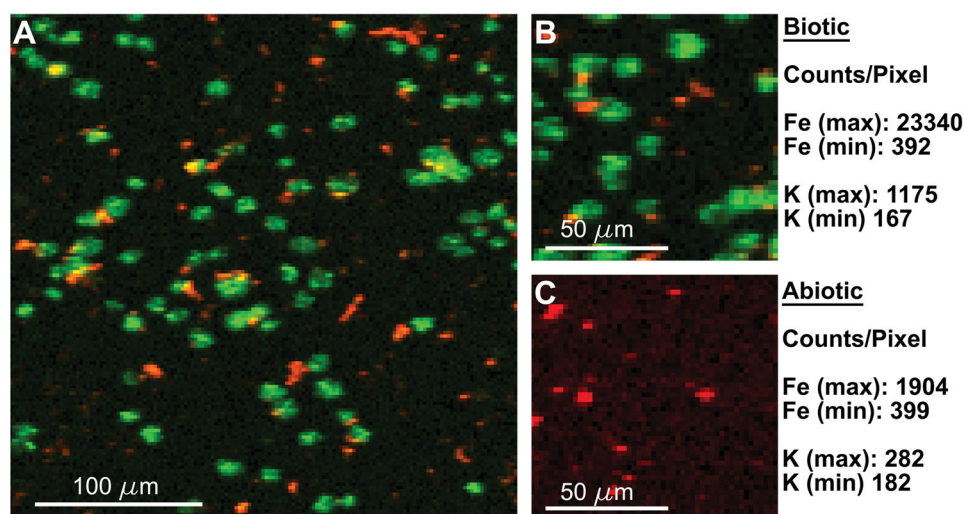
Figure 5. Synchrotron μXRF maps of Fe(Kα) (red) and K(Kα) (green) (for references to color see online version of figure). (A) Large area map of sample under biotic conditions on quartz. K concentrations reflect the positions of the algae cells, which are associated with Fe-precipitates. (B) and (C) Smaller area maps acquired with identical parameters for biotic and abiotic conditions on quartz. Note the difference in maximum counts per pixel of Fe intensities between abiotic and biotic conditions suggesting biologically enhanced Fe precipitation. In each case the brightest colors (red or green) represent the highest count rate measured, and black represents the lowest, with the scale shown for each figure. Note also that differences in fluorescence characteristics prevent direct concentration comparisons of Fe to K.

The co-location of secondary Fe-precipitates with the snow algae cells observed on quartz thin sections similarly supports the importance of the Fe-snow algae interactions (Figure 5).

Previous work has shown that the attachment of bacterial cells to Fe-containing minerals depends on the Fe-content in the mineral as well as microbial nutrient stress (Roberts 2004; Rogers and Bennett 2004). Harrold et al. (2018) also demonstrated that snow algae grow faster, are sustained for longer, and attain higher cell concentrations in the presence of Fe-containing forsterite under Fe-limited conditions. In these experiments, the oxidation state of the iron differs between the two Fe-containing minerals, olivine containing Fe^{2+}, and andradite containing Fe^{3+}. Previous studies indicate that 1) algae contain a ferric reductase in their cell wall (Eckhardt and Buckhout 1998; La Fontaine et al. 2002), 2) uptake of Fe includes a reductive step, and 3) the supply of ferrous Fe increased the rate of Fe uptake by the algae more than the supply of ferric Fe (Eckhardt and Buckhout 1998). The results here, with higher cell counts on the andradite surface even under lower concentrations in the medium (Figure 3), indicate the importance of the total amount of Fe in the mineral.

Bacteria may also play a role in the mobilization and utilization of mineral nutrients in snow algae blooms. The low algae concentrations and low algae:bacteria ratios in the epoxy-only condition (Table 2) indicate that the algae cells are much more strongly impacted by limiting iron than the bacteria (Table 2), consistent with the importance of iron for photosynthesis (Geider and La Roche 1994; Schoffman et al. 2016). Although algae have ferric reductase in their cell walls, which may contribute to iron transport and uptake (Eckhardt and Buckhout 1998; La Fontaine et al. 2002), bacterial mechanisms for Fe-uptake such as organic acid or siderophore release and mineral attachment (e.g., Song et al. 2007) may also contribute to the snow algae

blooms. Previous work on the culture used in this work (Harrold et al. 2018) indicated the presence of *Pseudomonas* and *Collimonas* species, which can participate in mineral weathering (Lapanje et al. 2012; Leveau et al. 2010; Uroz et al. 2009). Members of the *Pseudomonas* genus have also been shown to release siderophores and form biofilms under Fe-limiting conditions (Banin et al. 2005; Cornelis 2010; Loper and Henkels 1997; Vasil and Ochsner 1999; Yang et al. 2007). The bacteria present in these cultures and snow algae blooms in natural environments may therefore contribute to the success of snow algae blooms and the observed Fe-cycling.

Harrold et al. (2018) clearly showed that snow algae participate in iron cycling by enhancing the dissolution of forsterite. This study demonstrates that Fe-precipitation is greater in the presence of algal cells than in abiotic controls (Figure 5). Snow albedo is strongly decreased by the deposition of dust (Warren 1984), and it is possible that mineral dust alteration and the formation of secondary precipitates could impact snow albedo and melt rate. Therefore, in addition to enhancement of snow algae growth through nutrient delivery by dust deposition, snow algae may increase the formation of Fe-containing precipitates that further decrease snow albedo.

Conclusions

Both dust (Warren 1984) and snow algae (Benning et al. 2014; Kohshima et al. 1993; Lutz et al. 2014; Thomas and Duval 1995) strongly decrease the albedo of snow. Previous work has shown that minerals enhance snow algae growth in otherwise low-Fe systems (Harrold et al. 2018). We performed batch growth experiments with the snow algae *C. brevispina*, and the minerals andradite, forsterite, and quartz, to observe differences in attachment of snow algae to mineral surfaces. When low-Fe forsterite is present, the

number of snow algae on its surface increases with the concentration of snow algae in the medium. This result is consistent with the electrostatic attraction present between positively charged olivine and negatively charged snow algae cells at the pH (5.5) of our experiments. In contrast, the snow algae concentration present on the Fe-rich andradite remain high even when the concentration of snow algae in solution is greatly decreased. These results indicate that snow algae preferentially grow on Fe-rich surfaces. Additionally, μXRF measurements reveal that snow algae increase the formation of Fe-containing precipitates relative to abiotic controls. These results suggest that increased dust-on-snow deposition in a drying climate may lead to additional snow algal growth. Formation of Fe-containing precipitates by snow algae may further decrease snow albedo, resulting in a positive feedback loop that will likely exacerbate climate change.

Acknowledgements

Disclosure statement

Funding

ORCID

Charity M. Phillips-Lander   http://orcid.org/0000-0003-1064-8196
Elisabeth M. Hausrath   http://orcid.org/0000-0002-5520-1622

References

Achakulwisut P, Mickley LJ, Anenberg SC. 2018. Drought-sensitivity of fine dust in the US Southwest: implications for air quality and public health under future climate change. Environ Res Lett 13:054025.

Banin E, Vasil ML, Greenberg EP. 2005. Iron and *Pseudomonas aeruginosa* biofilm formation. P Natl Acad Sci USA 102:11076–11081.

Benning LG, Anesio AM, Lutz S, Tranter M. 2014. Biological impact on Greenland's Albedo. Nature Geosci 7:691–691.

Cornelis P. 2010. Iron uptake and metabolism in pseudomonads. Appl Microbiol Biotechnol 86:1637–1645.

Dewanti R, Wong ACL. 1995. Influence of culture conditions on biofilm formation by *Escherichia coli* O157:H7. Int J Food Microbiol 26:147–164.

Eckhardt U, Buckhout TJ. 1998. Iron assimilation in *Chlamydomonas reinhardtii* involves ferric reduction and is similar to Strategy I higher plants. J Exp Bot 49:1219–1226.

Ganey GQ, Loso MG, Burgess AB, Dial RJ. 2017. The role of microbes in snowmelt and radiative forcing on an Alaskan icefield. Nature Geosci 10:754–759.

Geider RJ, La Roche J. 1994. The role of iron in phytoplankton photosynthesis, and the potential for iron-limitation of primary productivity in the sea. Photosynth Res 39:275–301.

Hamilton TL, Havig J. 2017. Primary productivity of snow algae communities on stratovolcanoes of the Pacific Northwest. Geobiology 15:280–295.

Hamilton TL, Havig JR. 2018. Inorganic carbon addition stimulates snow algae primary productivity. Isme J 14:857–860.

Harrold ZR, Hausrath EM, Garcia AH, Murray AE, Tschauner O, Raymond JA, Huang S. 2018. Bioavailability of mineral-bound iron to a snow algal-bacterial coculture and implications for albedo-altering snow algal blooms. Appl Environ Microbiol 84:1–10.

Hausrath EM, Treiman AH, Vicenzi E, Bish DL, Blake D, Sarrazin P, Hoehler T, Midtkandal I, Steele A, Brantley SL, et al. 2008. Short- and long-term olivine weathering in svalbard: implications for mars. Astrobiology 8:1079–1092.

Hausrath EM, Brantley SL. 2010. Basalt and olivine dissolution under cold, salty, and acidic conditions: what can we learn about recent aqueous weathering on Mars? J Geophys Res 115:E12001.

Hausrath EM, Liermann LJ, House CH, Ferry JG, Brantley SL. 2007. The effect of methanogen growth on mineral substrates: will Ni markers of methanogen-based communities be detectable in the rock record? Geobiology 5:49–61.

Hausrath EM, Tschauner O. 2013. Natural fumarolic alteration of fluorapatite, olivine, and basaltic glass, and implications for habitable environments on mars. Astrobiology 13:1049–1064.

Havig JR, Hamilton TL. 2019. Snow algae drive productivity and weathering at volcanic rock-hosted glaciers. Geochim Cosmochim Acta 247:220–242.

Hisakawa N, Quistad SD, Hester ER, Martynova D, Maughan H, Sala E, Gavrilo MV, Rohwer F. 2015. Metagenomic and satellite analyses of red snow in the Russian Arctic. PeerJ 3:e1491.

Hodson AJ, Nowak A, Cook J, Sabacka M, Wharfe ES, Pearce DA, Convey P, Vieira G. 2017. Microbes influence the biogeochemical and optical properties of maritime Antarctic snow. J Geophys Res Biogeosci 122:1456–1470.

Hoham RW, Roemer SC, Mullet JE. 1979. The life history and ecology of the snow alga *Chloromonas brevispina* comb. nov. (Chlorophyta, Volvocales). Phycologia 18:55–70.

Hutchens E, Valsami-Jones E, Harouiya N, Chaïrat C, Oelkers EH, McEldoney S. 2006. An Experimental Investigation of the Effect of *Bacillus megaterium* on Apatite Dissolution. Geomicrobiol J 23:177–182.

Hutchens E. 2009. Microbial selectivity on mineral surfaces: possible implications for weathering processes. Fungal Biol Rev 23:115–121.

Jones DS, Lyon EH, Macalady JL. 2008. Geomicrobiology of biovermiculations from the Frasassi cave system, Italy. J Cave Karst Stud 702:78–93.

Jucker BA, Harms H, Zehnder AJ. 1996. Adhesion of the positively charged bacterium Stenotrophomonas (Xanthomonas) maltophilia 70401 to glass and Teflon. J Bacteriol 178:5472–5479.

Khalek MAA, Parekh BK. 2013. Reverse flotation of titanium carbide from garnet mineral using cationic surfactants. Int J Natural Sci Res 1:43–49.

Kohshima S, Seko K, Yoshimura Y. 1993. Biotic acceleration of glacier melting in Yala Glacier, Langtang Region, Nepal Himalaya. Snow and Glacier Hydrology 218:309–316.

La Fontaine S, Quinn JM, Nakamoto SS, Page MD, Göhre V, Moseley JL, Kropat J, Merchant S. 2002. Copper-dependent iron assimilation pathway in the model photosynthetic eukaryote *Chlamydomonas reinhardtii*. Eukaryotic Cell 1:736–757.

Lapanje A, Wimmersberger C, Furrer G, Brunner I, Frey B. 2012. Pattern of elemental release during the granite dissolution can be changed by aerobic heterotrophic bacterial strains isolated from Damma Glacier (Central Alps) deglaciated granite sand. Microb Ecol 63:865–882.

Leveau JHJ, Uroz S, De Boer W. 2010. The bacterial genus Collimonas: mycophagy, weathering and other adaptive solutions to life in oligotrophic soil environments. Environmental Microbiology 12:281–292.

Leya T, Rahn A, Lutz C, Remias D. 2009. Response of arctic snow and permafrost algae to high light and nitrogen stress by changes in pigment composition and applied aspects for biotechnology. FEMS microbiology ecology 67:432–443.

Liermann LJ, Hausrath EM, Anbar AD, Brantley SL. 2007. Assimilatory and dissimilatory processes of microorganisms affecting metals in the environment. J Anal at Spectrom 22:867–877.

Loper JE, Henkels MD. 1997. Availability of iron to Pseudomonas fluorescens in rhizosphere and bulk soil evaluated with an ice nucleation reporter gene. Appl Environ Microbiol 63:99–105.

Lutz S, Anesio AM, Villar SEJ, Benning LG. 2014. Variations of algal communities cause darkening of a Greenland glacier. FEMS Microbiol Ecol 89:402–414.

Lutz S, Anesio AM, Edwards A, Benning LG. 2015a. Microbial diversity on Icelandic glaciers and ice caps. Front Microbiol 6:307.

Lutz S, Anesio AM, Field K, Benning LG. 2015b. Integrated 'omics', targeted metabolite and single-cell analyses of Arctic snow algae functionality and adaptability. Front Microbiol 6:1323.

Lutz S, Anesio AM, Raiswell R, Edwards A, Newton RJ, Gill F, Benning LG. 2016. The biogeography of red snow microbiomes and their role in melting arctic glaciers. Nat Commun 7:11968.

Lutz S, Anesio AM, Edwards A, Benning LG. 2017. Linking microbial diversity and functionality of arctic glacial surface habitats. Environ Microbiol 19:551–565.

McAloon BP, Hofmeister AM. 1995. Single-crystal IR spectroscopy of grossular-andradite garnets. Am Mineral 80:1145–1156.

Pokrovsky OS, Schott J. 2000. Kinetics and mechanism of forsterite dissolution at 25 °C and pH from 1 to 12. Geochim Cosmochim Acta 64:3313–3325.

Roberts JA. 2004. Inhibition and enhancement of microbial surface colonization: the role of silicate composition. Chem Geol Bacteria Geochem Spec Metals 212:313–327.

Rogers JR, Bennett PC. 2004. Mineral stimulation of subsurface microorganisms: release of limiting nutrients from silicates. Chem Geol 203:91–108.

Schoffman H, Lis H, Shaked Y, Keren N. 2016. Iron-Nutrient Interactions within Phytoplankton. Front Plant Sci 7:1223–1223.

Song W, Ogawa N, Oguchi CT, Hatta T, Matsukura Y. 2007. Effect of Bacillus subtilis on granite weathering: a laboratory experiment. CATENA 70:275–281.

Stibal M, Box JE, Cameron KA, Langen PL, Yallop ML, Mottram RH, Khan AL, Molotch NP, Chrismas NAM, Calì Quaglia F, et al. 2017. Algae drive enhanced darkening of Bare Ice on the Greenland Ice Sheet. Geophys Res Lett 44:11,463–11,471.

Stumm W, Morgan JJ. 1981. Aquatic Chemistry: An Introduction Emphasizing Chemical Equilibria in Natural Waters New York: John Wiley & Sons, Inc., p780.

Suzuki I. 2001. Microbial leaching of metals from sulfide minerals. Biotechnol Adv 19:119–132.

Thomas WH, Duval B. 1995. Sierra Nevada, California, USA, snow algae: snow albedo changes, algal-bacterial interrelationships, and ultraviolet radiation effects. Arct Alp Res 27:389–399.

Uroz S, Calvaruso C, Turpault MP, Sarniguet A, de Boer W, Leveau JHJ, Frey-Klett P. 2009. Efficient mineral weathering is a distinctive functional trait of the bacterial genus Collimonas. Soil Biol Biochem 41:2178–2186.

Vasil ML, Ochsner UA. 1999. The response of Pseudomonas aeruginosa to iron: genetics, biochemistry and virulence. Mol Microbiol 34:399–413.

Warren SG. 1984. Impurities in snow: effects on Albedo and Snowmelt (Review). A Glaciology 5:177–179.

Wogelius RA, Walther JV. 1991. Olivine dissolution at 25 °C: effects of pH, CO_2, and organic acids. Geochim Cosmochim Acta 55:943–954.

Wogelius RA, Walther JV. 1992. Olivine dissolution kinetics at near-surface conditions. Chem. Geol. 97(1–2):101–112.

Yallop ML, Anesio AM, Perkins RG, Cook J, Telling J, Fagan D, MacFarlane J, Stibal M, Barker G, Bellas C, et al. 2012. Photophysiology and albedo-changing potential of the ice algal community on the surface of the Greenland ice sheet. Isme J 6:2302–2313.

Yang L, Barken KB, Skindersoe ME, Christensen AB, Givskov M, Tolker-Nielsen T. 2007. Effects of iron on DNA release and biofilm development by Pseudomonas aeruginosa. Microbiology 153:1318–1328.